Boosting of neuronal firing evoked with asynchronous and synchronous inputs to the dendrite

Hysell Oviedo and Alex D. Reyes

Center for Neural Science, New York University, 4 Washington Place, New York, New York 10003, USA
Correspondence and requests for materials should be addressed to A.D.R. (e-mail: reyes@cns.nyu.edu)

Published online: 11 February 2002, DOI: 10.1038/nn807

Dendritic conductances have previously been shown to boost excitatory postsynaptic potentials (EPSPs). To determine whether this boosting translates to an increase in the efficacy for evoking action potentials, we injected barrages of EPSPs that simulate the inputs generated by a population of presynaptic cells into either the dendrite or the soma of pyramidal neurons *in vitro*. Although the individual dendritic and somatic EPSPs were identical, barrages delivered to the dendrite generated much higher firing rates. Boosting occurred when the simulated cells fired asynchronously and synchronously. This Na^+-mediated boosting, which was manifested during repetitive firing, may compensate functionally for electrotonic attenuation of EPSPs.

Pyramidal neurons are the primary means by which signals processed in the cortex are transmitted to other parts of the CNS. Their dendrites can span all layers of cortex and contain thousands of synaptic inputs. The EPSPs from the many dendritic branches propagate to, and are integrated at, the soma and axon hillock, where they are transduced into action potentials[1–4]. Passive-cable models of dendrites predict that EPSPs reaching the action potential initiation region are severely attenuated because of electrotonic filtering[5–6]. This, in turn, suggests that the more distal synapses play a relatively minor role in influencing the cell's firing.

Attenuation of EPSPs is partly alleviated by voltage-dependent Na^+ and Ca^{2+} conductances in the dendrites[7–12]. Whether this subthreshold boosting extends to the suprathreshold range is not known. The uncertainty arises because many EPSPs are needed for the membrane potential to exceed the threshold for action potentials. The increase in the average membrane potential coupled with the presence of action potentials during a barrage of EPSPs alters the activation states not only of Na^+ and Ca^{2+} conductances but also of various K^+ and hyperpolarization-activated cation conductances in the dendrites, which may decrease firing[13–18]. Boosting of firing rate occurs only if the sum of all the ionic currents activated in the suprathreshold range is net inward.

Because dendritic conductances are time dependent, their effect on neuronal firing depends also on the timing of the presynaptic action potentials. Asynchronously firing presynaptic cells will evoke EPSPs that sum randomly to generate tonic depolarization. By contrast, synchronously firing presynaptic cells will evoke EPSPs that sum within a small time window to generate large voltage transients. Tonic depolarization will affect conductances with long time constants of activation or inactivation, whereas transients will affect primarily conductances with short time constants[19]. This property has been proposed to enhance the ability of neurons to detect synchronized inputs. The presence of strong K^+ conductances, for example, would shorten the effective membrane time constant and the integration time window such that only events that occur simultaneously would evoke action potentials[20–21].

We directly measured the effectiveness of dendritic and somatic inputs in cortical pyramidal neurons *in vitro*. Neurons were driven to fire with stimuli that mimicked inputs from a population of presynaptic cells firing repetitively. The simulated presynaptic cells were made to fire either asynchronously or synchronously to examine the response to a broad range of temporally correlated inputs and to test for specializations in the soma or dendrite[20] that might enhance the ability of neurons to encode input rate or timing[20,22–25]. As a result of Na^+ conductances, asynchronous and synchronous inputs delivered to the dendrite evoked substantially higher firing rates than those delivered to the soma. The greater effectiveness of dendritic inputs may offset electrotonic attenuation of EPSPs.

Results

We performed whole-cell recordings in the somata and apical dendrites of layer 5 pyramidal neurons in slices of sensorimotor cortex taken from postnatal day (P) 21–40 rats (unless otherwise specified). To simulate excitatory postsynaptic current (EPSC) generated by a single presynaptic cell, we injected time-varying current (**Fig. 1a**) into either the apical dendrite (I_d) or soma (I_s) through the recording electrodes[21]. We manually adjusted the parameters of the EPSCs (see Methods) so that when these were injected into the cell, the resultant voltage deflections at the soma ($E_{d\rightarrow s}$, $E_{s\rightarrow s}$) resembled unitary EPSPs (amplitude, 300–600 μV) recorded in layer 2/3 and layer 5 pyramidal neurons[26].

To mimic the inputs generated by a population of neurons, we simulated the activities of a specified number of presynaptic cells (N_{pre}; see Methods). Each simulated presynaptic cell fires repetitively at a specified rate (F_{pre}) to generate a train of EPSCs (**Fig. 1b**)[21]. The EPSC trains were summed and subsequently

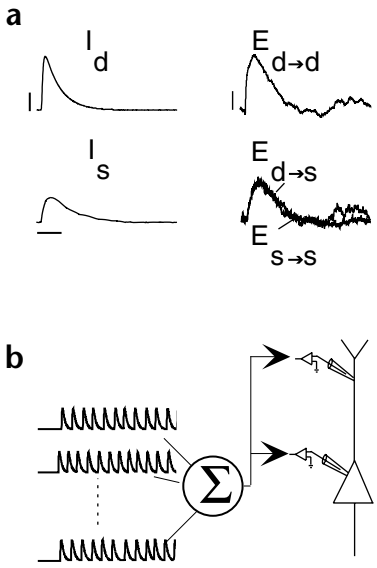

Fig. 1. Stimulus protocol. (**a**) EPSPs recorded at the dendrite ($E_{d\to d}$) and soma ($E_{s\to s}$) after current injection into the dendrite (I_d) and soma (I_s), respectively. $E_{d\to s}$ is $E_{d\to d}$ recorded with the somatic electrode. (**b**) EPSC trains were summed and injected into the cell. Vertical scale bars, 0.2 mV, 0.02 nA. Horizontal scale bar, 20 ms.

injected through either recording electrode. Because the EPSCs were summed linearly and were injected under current clamp, the protocol mimics best the condition in which synaptic inputs from electrotonically distant and spatially disparate locations throughout the dendritic tree converge at a common site at either a mother branch (at the site of the dendritic recording) or the soma. Under this condition, mutual shunting and changes in the driving force of the EPSCs are minimal and summation is linear[5]. Consequently, any nonlinearities introduced by dendritic conductances at the sites of convergence can be examined exclusively.

To examine the responses of neurons to inputs with a broad range of temporal correlations, we made the simulated presynaptic cells fire asynchronously and synchronously. In the asynchronous mode, we added jitter to the simulated action-potential trains to remove temporal correlation between the presynaptic cells (see Methods). This generated a predominantly steady current (**Fig. 2a**, lower trace), which was then injected into the soma. Increasing the EPSC rate ($N_{pre}\times F_{pre}$) led the neuron eventually to fire repetitively (**Fig. 2a**, upper trace). The mean (±s.d.) firing rate (taken from 20 trials) plotted against the EPSC rate (**Fig. 2b**) shows that identical firing rates were obtained whether the EPSC rate was varied by changing N_{pre} and keeping F_{pre} constant or vice versa. The firing rate can therefore be approximated by equation (1):

$$F = k\times F_{pre}\times N_{pre}\times A = k\times \text{EPSC rate}\times A \qquad (1)$$

where k is the slope and A is the total charge (equal to the area under an individual EPSC). Because the product of EPSC rate and A gives the average current (**Fig. 2b**, upper abscissa), k is the slope of a frequency–current plot obtained by injecting a series of current steps into the soma[1,4].

In the synchronous mode, a specified subset of the simulated cells fired identically during the second half of the stimulus train (**Fig. 2c**, synch). This resulted in large composite EPSCs that occurred repetitively at a rate equal to F_{pre}. Both N_{pre} and F_{pre} were kept constant. Systematically increasing the proportion of synchronized N_{pre} cells increased the coefficient of variation of the injected current (**Fig. 2d**, upper abscissa) and had pronounced effects on neuronal firing. Synchronizing a small number of presynaptic cells (**Fig. 2c**, upper trace; 20% of 150 N_{pre}) caused the firing to become more irregular (compare asynchronous with synchronous). With a further increase in synchrony, one action potential occurred per EPSC cycle (data not shown). In 5 out of 13 neurons, 2 to 3 action potentials were evoked per cycle at 100% synchrony (**Fig. 2c**, lower traces). These changes in patterns were accompanied by changes in firing rate ($n = 13$). The firing rate (for the neuron shown in **Fig. 2d**) dipped to 20 Hz (F_{pre}) as the action potentials became perfectly phase locked to the EPSCs and peaked at 40 Hz with 100% synchrony. Although the firing rates of all cells tested varied with the level of synchrony, the shape of the curve depended on the values of N_{pre} and F_{pre} (H.O. and A.D.R., unpublished observations).

To determine whether inputs to other compartments generated comparable responses, we made simultaneous recordings at the soma and the apical dendrite (100–300 μm from the soma). We manually adjusted the EPSCs injected into the dendrite (I_d; **Fig. 1a**) and soma (I_s) so that the resultant average EPSPs measured with the somatic electrode ($E_{d\to s}$, $E_{s\to s}$) were identical. In general, larger and briefer EPSCs injected into the dendrite were

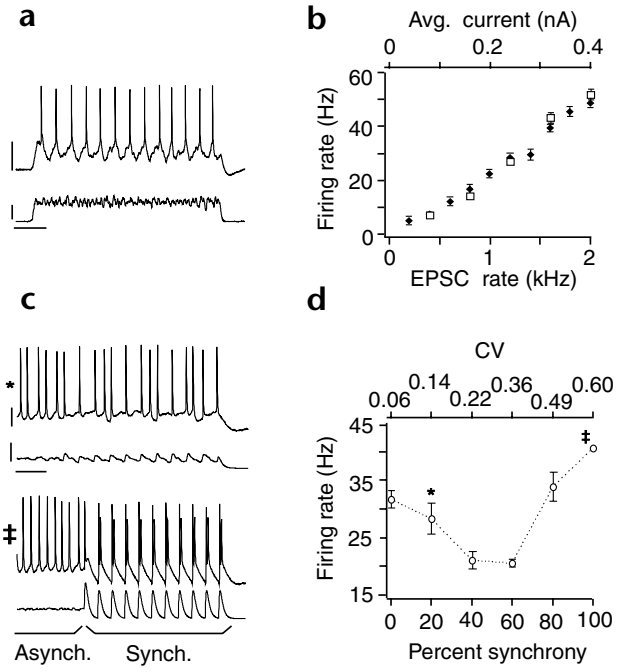

Fig. 2. Response to somatic injection. (**a**) Injected current (bottom) and associated firing (top) when the EPSCs were delivered asynchronously. (**b**) Plot of average firing rate (±s.d.) versus EPSC rate. EPSC rate was varied either by changing N_{pre} (filled diamonds) or F_{pre} (open squares). Average injected current is shown on the top abscissa. (**c**) Firing evoked when 20% (*) and 100% (‡) of the EPSCs were introduced synchronously (synch.) during the last half of the stimulus train. (**d**) Average firing rate (±s.d.) plotted against percent synchrony. The coefficient of variation of the injected current is shown on the upper abscissa. Representative voltage traces for points marked by * and ‡ are shown in (**c**). N_{pre} = 150; F_{pre} = 20 Hz. Vertical scale bars for (**a**, **c**): 20 mV, 0.2 nA. Horizontal scale bars: 200 ms for (**a**), 100 ms for (**c**).

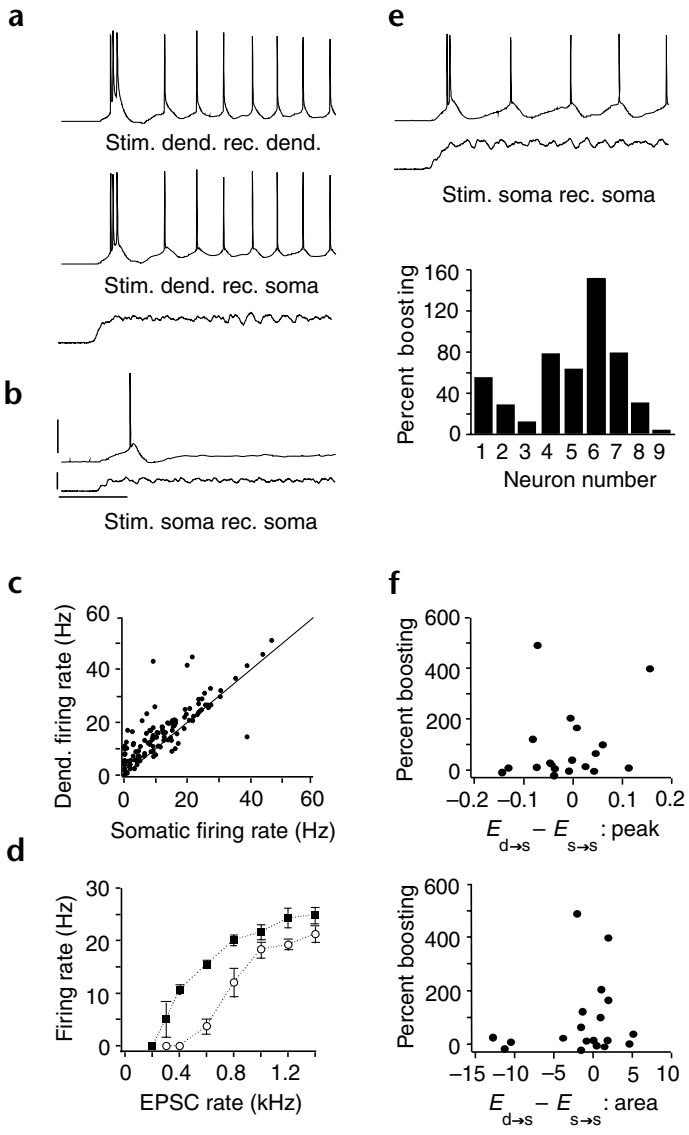

Fig. 3. Response to asynchronous dendritic stimulation. (**a**) Current injected into the dendrite (third trace) and action potentials recorded simultaneously with the dendritic (first trace) and somatic (second trace) electrodes. (**b**) Current injected into the soma (lower trace) and action potentials recorded with the somatic electrode (upper trace). (**c**) The firing rate (mean ± s.d.) evoked during dendritic stimulation is plotted against that evoked during somatic stimulation. (**d**) Plot of average (±s.d.) firing rate versus EPSC rate for one cell. Stimuli were delivered at either the dendrite (filled squares) or the soma (open circles). (**e**) Firing evoked (upper trace) when the current injected into the soma (lower trace) was equal to that injected into the dendrite (third trace in **a**). The bottom graph shows the percentage of dendritic boosting ($100 \times (F_d - F_s)/F_s$) for 9 cases where the average currents injected into the dendrite and soma were equal. (**f**) Percent boosting plotted against the differences between the peak amplitudes (top) and between the areas (bottom) of $E_{d\to s}$ and $E_{s\to s}$. Scale bars for (**a**, **b**, **e**): 20 mV, 0.2 nA, 200 ms.

necessary to compensate for the filtering of dendritic EPSPs ($E_{d\to d}$)[6]. With this normalization procedure, the depolarizations near the soma and action potential–initiation region were equal for both dendritic and somatic injections; only the location of the inputs differed. A similar process occurs naturally in hippocampal pyramidal neurons[27]. In these cells, the magnitudes of synaptic conductances increase systematically along the somatodendritic axis such that the EPSPs recorded at the soma have comparable amplitudes independent of their dendritic origin.

Asynchronous dendritic stimulation (**Fig. 3a**) consistently evoked higher firing rates than somatic stimulation (**Fig. 3b**). A plot of dendritically evoked versus somatically evoked firing rates (**Fig. 3c**; $n = 23$ cells) showed that most data points were above the unitary slope line. A comparison of somatic and dendritic voltage traces indicated that action potentials were initiated in the dendrites in only 3 out of 23 neurons (data not shown). Boosting of firing rate did not vary systematically with the age of the rats (P21–40) and occurred in 6 of 8 neurons from rats as young as P12–14.

A plot of firing rate versus EPSC rate for one cell (**Fig. 3d**) showed that the greatest difference in firing rates between dendritic (filled squares) and somatic (open circles) stimulation occurred at low EPSC rates; at higher rates, each curve asymptotically approached a maximum firing rate. In general, the curves did not superimpose if one was shifted along the horizontal axis, but the difference between the slopes of the linear portion of the curves was not significant ($p = 0.11$; $n = 14$; paired t-test).

Boosting of firing rate was not simply due to the fact that larger-amplitude currents were injected into the dendrite. The firing rate evoked with dendritic injection (F_d) was consistently higher than that evoked with somatic injection (F_s), even when the average currents injected into both compartments were equal (**Fig. 3a** and **e**). We calculated the percentage increase in firing rate attributable to dendritic processes (equal to $100 \times (F_d - F_s)/F_s$) for nine cases in which the average currents injected into the dendrite and soma were equal (**Fig. 3e**, bottom graph). The difference in firing rate between dendritic and somatic injection was significant ($p = 0.005$; paired t-test).

To exclude the possibility that the observed boosting was due to imperfect matching of $E_{d\to s}$ and $E_{s\to s}$, we plotted the percent boosting against the differences between the peak amplitudes and between the areas of $E_{d\to s}$ and $E_{s\to s}$ (**Fig. 3f**). The percent boosting was not significantly correlated with either parameter (peak, $r = 0.237$, $p = 0.327$; area, $r = 0.185$, $p = 0.448$; $n = 19$). We obtained similar results when we placed a third electrode that was dedicated to voltage recording at the soma ($n = 5$; data not shown). This eliminated measurement errors associated with using one electrode for voltage recording and current injection.

The firing rate during synchronous stimulation at the dendrite was similarly enhanced ($n = 7$; **Fig. 4a**). As with somatic stimulation, the average firing rate evoked with dendritic stimulation varied systematically with the level of synchrony (**Fig. 4b**). There were no obvious differences in the degree to which synchronous or asynchronous inputs were boosted. The difference in firing rates between dendritic and somatic stimulation ($F_d - F_s$) at 0% synchrony was not significantly different from that at 100% synchrony ($p = 0.10$; $n = 8$; paired t-test). The depth of the modulation (equal to the difference between the maximum and minimum firing rates as synchrony was increased) tended to be greater for dendritic (17 ± 15 Hz; mean ± s.d.) than for somatic (8 ± 6 Hz) stimulation, although again the difference was not statistically significant ($p = 0.12$; $n = 8$; paired t-test). These results indicate

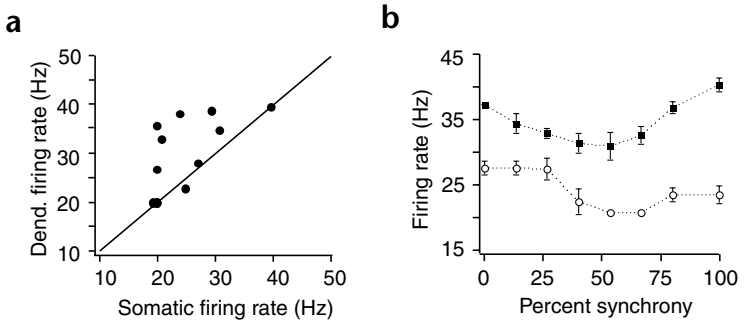

Fig. 4. Responses to synchronous dendritic stimulation. (**a**) Average (±s.d.) firing rate evoked with dendritic stimulation plotted against that evoked with somatic stimulation. (**b**) Plot of average (±s.d.) firing rate versus percent synchrony for stimuli delivered at the dendrite (filled squares) and soma (open circles) for one neuron. N_{pre} = 50; F_{pre} = 20 Hz.

that the responses to synchronous inputs at the dendrites are not enhanced preferentially over asynchronous inputs.

To determine whether persistent Na^+ conductances in the dendrites contributed to boosting[7,9,28], we delivered the Na^+-channel blocker tetrodotoxin (TTX, 100 nM) exclusively to the dendrite through a pipette. $E_{d\to s}$ and $E_{s\to s}$ were adjusted to be equal before the application of TTX. In the presence of TTX, the firing rates evoked with asynchronous dendritic current injection decreased (**Fig. 5a** and **b**, left traces; $n = 10$) to a level equal to the somatically evoked firing rate (**Fig. 5c**). We confirmed that TTX blocked exclusively the Na^+ conductances in the dendrite by recording at the soma and dendrite the action potential that was evoked with somatic current injection (**Fig. 5a** and **b**, right traces; $n = 10$). In all cases, only the dendritic action potential was blocked. A comparison of dendritic and somatic firing both before (control; F_C) and during (F_{TTX}) TTX application showed that only the dendritically evoked firing was affected by TTX (quantified as the percentage change in firing rate or $100 \times (F_C - F_{TTX})/F_C$; **Fig. 5d**). Thus, boosting of firing rates can be accounted for mainly by activation of local dendritic Na^+ conductances.

Discussion

As a result of dendritic Na^+ conductances, the firing evoked with inputs at the dendrite is greater than that of inputs at the soma. The dendritic boosting of firing occurred for inputs with a wide range of temporal correlations and occurred despite the fact that the dendritically and somatically injected EPSCs were adjusted so that the EPSPs at the soma were of equal amplitudes. It is unlikely that boosting of dendritic input resulted from the way we performed the EPSP normalization (**Fig. 1a**). A parsimonious explanation is that the dendrites act as a low-pass filter so that transient inputs (such as individual EPSPs) are attenuated more than tonic inputs (as would occur during a barrage of EPSPs; **Fig. 3a**)[5–6]. As a result, the total drive to the soma during a barrage of inputs into the dendrite may be greater than that predicted from the sum of the individual EPSPs reaching the soma. Three lines of evidence suggest, however, that at the sites of the dendritic recordings this effect constitutes a relatively small portion of the overall boosting. First, boosting occurred even when the average current injected into the dendrite was equal to that injected into the soma (**Fig. 3e**). In such a case, the average current reaching the soma from the dendrite (in a passive neuron) should be less than or equal to the average current that was injected into the soma. Second, boosting occurred even during synchronous stimulation (**Fig. 4**). During synchrony, the current injected into the dendrite consists of transients (**Fig. 2c**). Finally, application of TTX exclusively to the dendrite blocked boosting of firing (**Fig. 5**).

One of the more notable results is that the effectiveness of synaptic inputs at evoking firing cannot be reliably predicted from the parameters of individual subthreshold EPSPs. In another study[28], Na^+ conductances in the dendrites contributed relatively little to the amplitudes of EPSPs injected individually. The apparent discrepancy between those results and ours can be accounted for by the fact that a population of EPSPs generates larger and longer-lasting depolarizations, both of which would increase activation of the persistent Na^+ conductance[20]. Therefore, the boosting effects of Na^+ may become more prominent when a sufficient number of EPSPs arrive to evoke repetitive firing.

Increased firing rates with dendritic stimulation occurred for both asynchronous and synchronous stimulation, indicating that the result can be generalized for a broad class of inputs. The evoked firing during asynchronous and synchronous inputs reflects different aspects of the input signal. During asynchronous stimulation, the evoked firing rate is monotonically related to, and hence encodes, input rate (equation 1). During synchronous stimulation, the firing rate varied with the level of synchrony and did not accurately reflect input rate because N_{pre} and F_{pre} were kept constant. At the sites of our dendritic recordings, we found no

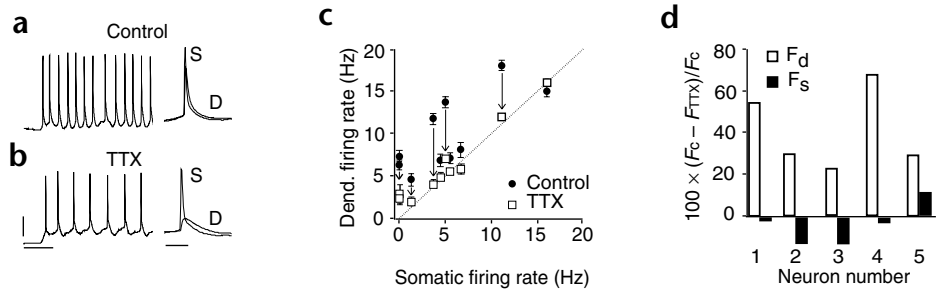

Fig. 5. Role of dendritic Na^+ conductances. (**a**) Firing evoked at soma (left) when an asynchronous stimulus was delivered at the dendrite. (**b**) Firing evoked during application of TTX at the dendrite. Traces at right show action potentials recorded simultaneously at the soma (S) and dendrite (D) when the stimulus was delivered at the soma. (**c**) Plot of average (±s.d.) firing rates evoked with dendritic stimulation versus those evoked with somatic stimulation ($n = 10$). Dendritic firing rates are shown before (filled circles) and during (open squares) application of TTX. (**d**) Percent change in firing rate for dendritic (open squares) and somatic (filled squares) stimulation in the presence of TTX. Vertical scale bars for (**a**, **b**), 20 mV. Horizontal scale bars, 200 ms and 20 ms for left and right traces, respectively.

evidence that the dendrites are specialized for detecting synchronous events. We cannot exclude the possibility that such specializations exist at other parts of the dendritic tree, however.

Boosting of firing rate by dendritic Na^+ conductances may occur as follows. When a population of presynaptic cells becomes active, the synaptic current that is generated at the dendrites propagates to the soma and the action potential initiation region to initiate a sequence of events leading to repetitive firing[1,4]. At the sites of the dendritic stimulation (100–300 μm from the soma), the action potentials are probably evoked first at the axon hillock and then at the soma and dendrite[2–3]. The firing rate is proportional to the magnitude of the synaptic current reaching the soma[4]. The depolarization caused by the EPSP barrage activates the persistent Na^+ conductances in the dendrite and the resultant inward current sums with the synaptic current to increase the overall drive to the soma. In cases where the dendritically and somatically injected currents are equal, the higher input resistance of the dendrite probably causes a larger local synaptic depolarization and hence allows greater activation of Na^+ conductances.

In addition to Na^+ conductances, the dendrites of pyramidal neurons contain Ca^{2+}, K^+ and hyperpolarization-activated cation conductances[12–18]. All of these affect the shape of subthreshold EPSPs. As with Na^+ conductances, their activation states are likely to change with a barrage of inputs and are thus likely to influence the resultant firing. At the site of our dendritic recordings, Na^+ conductances predominate and boosting occurs. However, the fact that there are gradients in the distribution and biophysical properties of conductances along the somatodendritic axis[14–16,29–30] suggests that boosting of firing rate, and hence the effectiveness of dendritic input, may vary throughout the entire dendritic tree.

Methods

Surgical and slicing techniques[2,26] followed guidelines set forth by New York University's Animal Welfare Committee. Briefly, we anesthetized Wistar rats with halothane and decapitated them. We excised one hemisphere of the brain, glued it to a slicing chamber and immersed it in ice-cold, oxygenated artificial cerebrospinal fluid (125 mM NaCl, 2.5 mM KCl, 25 mM glucose, 25 mM $NaHCO_3$, 1.25 mM NaH_2PO_4, 2 mM $CaCl_2$ and 1 mM $MgCl_2$). We used a vibratome slicer to make parasaggital (300 μm thick) slices cut at a 30° angle from the horizontal plane. We stored the slices in a holding chamber at 35°C for 30 min and at room temperature thereafter. We transferred individual slices to a recording chamber mounted on an upright microscope and perfused them with artificial cerebrospinal fluid heated to 33–34°C. We identified layer 5 pyramidal neurons with the aid of infrared, differential interference contrast videomicroscopy. We performed whole-cell current-clamp recordings using borosilicate microelectrodes pulled to diameters of 2 μm and 1 μm for somatic and dendritic recordings, respectively. Somatic and dendritic electrodes had direct current resistances of 5–20 MΩ and 30–40 MΩ , respectively, when filled with 100 mM potassium gluconate, 20 mM KCl, 4 mM MgATP, 10 mM phosphocreatine, 0.3 mM GTP and 10 mM HEPES. We filtered voltage and current signals at 10 kHz and digitized them at 2–10 kHz.

We stimulated neurons with inputs designed to mimic the net synaptic current generated when a population of presynaptic cells fire. We used a computer program to simulate the activities of a specified number of presynaptic cells (N_{pre}). Each simulated cell fired repetitively for 1 s at a specified average rate (F_{pre}). We added jitter to the interspike intervals such that they were distributed normally about a mean interval with a standard deviation of ±10%. In the asynchronous mode, all the neurons fired independently with respect to each other. To eliminate temporal correlation between the neurons, we distributed the start times of the spike trains uniformly within one interspike interval. In the synchronous mode, we removed the random delay in the start time and the jitter in the interspike intervals such that the discharge patterns of a specified number of simulated neurons were identical.

Each time a simulated cell fired an action potential, an associated synaptic current was calculated. The time course of the current (**Fig. 1a**) was described by $I(t) = m(1 - e^{-t/\tau 0})e^{-t/\tau 1}$, where m is the amplitude and $\tau 0$ and $\tau 1$ are time constants. The following procedure was used to match $E_{d\to s}$ with $E_{s\to s}$. We injected I_s into the soma and compiled an average of $E_{s\to s}$ from 20–30 sweeps. We manually adjusted the three free parameters and re-injected I_s until the average $E_{s\to s}$ resembled unitary EPSPs recorded in previous experiments[26]. We then injected I_d into the dendrite and compiled the average $E_{d\to s}$ (recorded with the somatic electrode) and overlaid it with the average $E_{s\to s}$. We adjusted the parameters until the average $E_{d\to s}$ matched $E_{s\to s}$ (**Fig. 1**). We convolved the current with the spike trains of each presynaptic cell[21]. We summed the current trains from all the presynaptic cells, converted the summed current to an analog signal and injected it into the cell through the amplifier and recording electrode. We delivered stimuli at >3-s intervals to ensure that the cells reached resting conditions after each stimulus.

Acknowledgements

The authors thank L. Abbott, F. Chance, A. Movshon and J. Rinzel for providing helpful comments. This work was supported by NSF grant IBN-0079619 (A.D.R.) and by an NSF Minority Fellowship (H.O.).

Competing interests statement

The authors declare that they have no competing financial interests.

RECEIVED 11 DECEMBER 2001; ACCEPTED 14 JANUARY 2002

1. Granit, R., Kernell, D. & Lamarre, Y. Algebraical summation in synaptic activation of motoneurones firing within the 'primary range' to injected currents. *J. Physiol. (Lond.)* **187**, 379–399 (1966).
2. Stuart, G. & Sakmann, B. Active propagation of somatic action potentials into neocortical pyramidal cell dendrites. *Nature* **367**, 69–72 (1994).
3. Colbert, M. & Johnston, D. Axonal action potential initiation and Na^+ channel densities in the soma and axon initial segment of subicular pyramidal neurons. *J. Neurosci.* **16**, 6676–6686 (1996).
4. Schwindt, P. & Crill, W. Equivalence of amplified current flowing from dendrite to soma measured by alteration of repetitive firing and by voltage clamp in layer 5 pyramidal neurons. *J. Neurophysiol.* **76**, 3731–3739 (1996).
5. Rall, W. Theoretical significance of dendritic trees for neuronal input-output relations. in *Neural Theory and Modeling* (ed. Reiss, R. F.) 73–97 (Stanford Univ. Press, Palo Alto, California, 1964).
6. Stuart, G. & Spruston, N. Determinants of voltage attenuation in neocortical pyramidal neuron dendrites. *J. Neurosci.* **18**, 3501–3510 (1998).
7. Schwindt, P. & Crill, W. Amplification of synaptic current by persistent sodium conductance in apical dendrite of neocortical neurons. *J. Neurophysiol.* **74**, 2220–2224 (1995).
8. Magee, J. C. & Johnston, D. Synaptic activation of voltage-gated channels in the dendrites of hippocampal pyramidal neurons. *Science* **268**, 301–304 (1995).
9. Lipowsky, R., Gillessen, T. & Alzheimer, C. Dendritic Na^+ channels amplify EPSPs in hippocampal CA1 pyramidal cells. *J. Neurophysiol.* **76**, 2181–2191 (1996).
10. Gillessen, T. & Alzheimer, C. Amplification of EPSPs by low Ni^{2+}- and amilioride-sensitive Ca^{2+} channels in apical dendrites of rat CA1 pyramidal neurons. *J. Neurophysiol.* **77**, 1639–1643 (1997).
11. Schiller, J., Schiller, Y., Stuart, G. & Sakmann, B. Calcium action potentials restricted to distal apical dendrites of rat neocortical pyramidal neurons. *J. Physiol. (Lond.)* **505**, 605–616 (1997).
12. Zhu, J. J. Maturation of layer 5 neocortical pyramidal neurons: amplifying salient layer 1 and layer 4 inputs by Ca^{2+} action potentials in adult rat tuft dendrites. *J. Physiol. (Lond.)* **526**, 571–587 (2000).
13. Kang, J., Huguenard, J. R. & Prince, D. A. Development of BK channels in neocortical pyramidal neurons. *J. Neurophysiol.* **76**, 188–198 (1996).
14. Magee, J. C. Dendritic hyperpolarization-activated currents modify the integrative properties of hippocampal CA1 pyramidal neurons. *J. Neurosci.* **18**, 7613–7624 (1998).
15. Poolos, N. P. & Johnston, D. Calcium-activated potassium conductances contribute to action potential repolarization at the soma but not the dendrites of hippocampal CA1 pyramidal neurons. *J. Neurosci.* **19**, 5205–5212 (1999).
16. Bekkers, J. M. Distribution and activation of voltage-gated potassium channels in cell-attached and outside-out patches from large layer 5 cortical pyramidal neurons of the rat. *J. Physiol. (Lond.)* **525**, 611–620 (2000).
17. Korngreen, A. & Sakmann, B. Voltage-gated K^+ channels in layer 5

neocortical pyramidal neurones from young rats: subtypes and gradients. *J. Physiol. (Lond.)* **525**, 621–639 (2000).
18. Williams, S. R. & Stuart, G. J. Site independence of EPSP time course is mediated by dendritic I_h in neocortical pyramidal neurons. *J. Neurophysiol.* **83**, 3177–3182 (2000).
19. Reyes, A. D. Influence of dendritic conductances on the input-output properties of neurons. *Annu. Rev. Neurosci.* **24**, 653–675 (2001).
20. Softky, W. Sub-millisecond coincidence detection in active dendritic trees. *Neuroscience* **58**, 13–41 (1994).
21. Reyes, A. D., Rubel, E. W. & Spain, W. J. *In vitro* analysis of optimal stimuli for phase-locking and time-delayed modulation of firing in avian nucleus laminaris neurons. *J. Neurosci.* **16**, 993–1007 (1996).
22. Ferster, D. & Spruston, N. Cracking the neuronal code. *Science* **270**, 756–757 (1995).
23. Shadlen, M. N. & Newsome, W. T. The variable discharge of cortical neurons: implications for connectivity, computation, and information coding. *J. Neurosci.* **18**, 3870–3896 (1998).
24. Borst, A. & Theunissen, F. E. Information theory and neural coding. *Nature Neurosci.* **2**, 947–957 (1999).
25. Stevens, C. F. & Zador, A. M. Input synchrony and the irregular firing of cortical neurons. *Nature Neurosci.* **1**, 210–217 (1998).
26. Reyes, A. D. & Sakmann, B. Developmental switch in the short-term modification of unitary EPSPs evoked in layer 2/3 and layer 5 pyramidal neurons of rat neocortex. *J. Neurosci.* **19**, 3827–3835 (1999).
27. Magee, J. C. & Cook, E. P. Somatic EPSP amplitude is independent of synapse location in hippocampal pyramidal neurons. *Nature Neurosci.* **3**, 895–903 (2000).
28. Stuart, G. & Sakmann, B. Amplification of EPSPs by axosomatic sodium channels in neocortical pyramidal neurons. *Neuron* **15**, 1065–1076 (1995).
29. Colbert, C. M., Magee, J. C., Hoffman, D. A. & Johnston, D. Slow recovery from inactivation of Na^+ channels underlies the activity-dependent attenuation of dendritic action potentials in hippocampal CA1 pyramidal neurons. *J. Neurosci.* **17**, 6512–6521 (1997).
30. Mickus, T., Jung, H. Y. & Spruston, N. Properties of slow, cumulative sodium channel inactivation in rat hippocampal CA1 pyramidal neurons. *Biophys. J.* **76**, 846–860 (1999).